Heliyon 9 (2023) e16143

Contents lists available at ScienceDirect

Heliyon

journal homepage: www.cell.com/heliyon

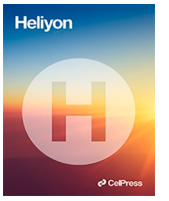

Research article

RNAseq analysis of the drug jian-yan-ling (JYL) using both in vivo and in vitro models

Xiaobo Zhang [a,1], Yunliang Zhai [b,1], Dandan Zhang [b], Chang Che [c], Yayun Zhang [b], Quan Li [b], Xue Zhang [b], Lingrui Zhao [c,*]

[a] *School of Life Sciences, Fudan University, Shanghai, 200438, China*
[b] *Lei Yun Shang Pharmaceutical Group Co.,Ltd., Suzhou, 215009, China*
[c] *Key Laboratory of Growth Regulation and Translational Research of Zhejiang Province, School of Life Sciences, Westlake University, Hangzhou, 310024, China*

ARTICLE INFO

Keywords:
Jian-yan-ling (JYL) drug
RNA sequencing
Drosophila melanogaster
HL60 cell line
Protein ubiquitination decomposition
anti-aging

ABSTRACT

Ethnopharmacological relevance: Jian-yan-ling (JYL) is a drug used in traditional Chinese medicine (TCM) prescriptions for the treatment of tumors after radiotherapy and chemotherapy, to effectively alleviate leukocytopenia. However, the genetic mechanisms underlying the function of JYL remain unclear.

Aim of the study: This study aimed to explore the RNA changes and potential biological processes related to the anti-aging or life-extending effects of JYL treatments.

Materials and methods: In vivo treatments were performed using Canton-S *Drosophila* corresponding to three groups: control, low-concentration (low-conc.), and high-concentration (high-conc.) groups. The low-conc. And the high-conc. Groups were treated with 4 mg/mL JYL and 8 mg/mL JYL, respectively. Thirty *Drosophila* eggs were placed in each vial, and the third instar larvae and adults 7 and 21 days post-eclosion were collected for RNA sequencing, irrespective of the gender.

In vitro treatments were conducted using humanized immune cell lines HL60 and Jurkat, which were divided into 3 groups: control (0 μg/mL JYL), low-concentration (40 μg/mL JYL), and high-concentration (80 μg/mL JYL). The cells were collected after 48 h of each JYL drug treatment. Both the *Drosophila* and cell samples were analyzed using RNA sequencing.

Results: The in vivo experiments revealed 74 upregulated genes in the low-concentration group, and CG13078 was a commonly downregulated differential gene, which is involved in ascorbate iron reductase activity. Further analysis of the co-expression map identified the key genes: regulatory particle non-ATPase (RPN), regulatory particle triple-A ATPase (RPT), and tripeptidyl-peptidase II (TPP II). For the in vitro experiments, 19 co-differential genes were compared between different concentrations of the HL 60 cell line, of which three genes were upregulated: LOC107987457 (phostensin-like gene), HSPA1A (heat shock protein family A member 1 A), and H2AC19 (H2A clustered histone 19). In the HL 60 cell line, JYL activated proteasome-related functions. In the Jurkat cell line, there were no common differential genes despite the presence of a dosage-dependent trend.

* Corresponding author.
E-mail address: zhaolingrui@westlake.edu.cn (L. Zhao).
[1] These authors contributed equally: Xiaobo Zhang, Yunliang Zhai.

https://doi.org/10.1016/j.heliyon.2023.e16143
Received 11 August 2022; Received in revised form 21 April 2023; Accepted 6 May 2023
Available online 19 May 2023

Conclusions: The RNA-seq results showed that the traditional Chinese medicine JYL has longevity and anti-aging effects, indicating that further investigation is required.

1. Introduction

The modern development of ancient Chinese medicines is embodied by traditional Chinese medicine (TCM) prescriptions. Historically, the use of Western medicines has increased, as inferred from the evidence provided by quantitative and standardized analyses, while the use of TCM prescriptions has also increased due to the accumulation of evidence showing their curative effects and independent folk collections (including traditional Chinese medical books and prescriptions transmitted by word of mouth) and compilations. There is consequently a need to improve our understanding of TCM treatments using current scientific techniques, such as our rapidly developing genetic technologies. TCM prescriptions have been successfully utilized for thousands of years to treat various diseases. For instance, artemisinin and its derivatives, an extract from *Artemisia annua*, are front-line antimalarial drugs known for their efficacy and low toxicity [23]. Although artemisinin is the standard treatment for malaria, its underlying genetic mechanisms remain poorly understood. Western medicines are developed based on one or a few active compounds, to influence several specific biologically activity targets or pathways, so their pharmacological functions can be determined with relative ease. In contrast, TCM prescriptions contain multiple active compounds. The "multi-component, multi-target" nature of TCM prescriptions poses a challenge when trying to elucidate their underlying molecular mechanisms (see Fig. 7).

In recent years, with the development of high-throughput technologies and innovative computational methods in drug discovery, the desire to elucidate the molecular mechanisms of TCM have been reinvigorated. Pharmacotranscriptomes have become a powerful tool by which to evaluate drug TCM drug efficacy and discover new drug targets that are based on several pivotal consensuses: gene expression can be accurately measured and could potentially be a "universal language" for disease characterization and prediction [24]; gene expression can link different biological states and systems [4]; different biological pathways can drive different disease phenotypes. Thus, TCM prescription research has increasingly turned to high-throughput transcriptome screening to understand their molecular effects and components. Many studies have examined the genetic targets of herbs and ingredients and linked them to various diseases.

The Integrated Database of Traditional Chinese Medicine (TCMID) was first established in 2013 with the aim of creating a comprehensive database for the digitization and standardization of TCM [24]. This has been recognized by pharmacists and Chinese medicine researchers. TCMID 2.0 was later updated in 2017 with data relating to 18 203 TC M ingredients, 15 prescriptions, 82 related targets, 1356 drugs, 842 diseases, and various associations among the data. Considering that chemical changes may occur after the formula is decocted or boiled, new data were collected based on the composition of the formula after the processing steps. Meanwhile, 3895 mass spectrometry (MS) data points for 729 Chinese herbs were added as supplementary materials for ingredient identification. TCMID 2.0 will further promote the modernization of TCM and facilitate the exploration of their underlying biological processes. HERB [4], another Chinese medicine database for high-throughput experimental references, was recently established in 2020. In HERB, 6164 gene expression profiles were reanalyzed from 1037 high-throughput TCM and ingredient evaluation experiments, connections between these TCM, and 2837 modern medicines were generated by mapping the complete TCM transcriptome data set to the largest data set of modern medicines, the CMap. In addition, HERB screened 1241 novel genetic targets for 473 herbs and 494 modern diseases from 1966 recently published articles. As a result, 12 933 genetic targets and 28 212 diseases were identified as associated with 7263 TC M and 49 258 chemical components. HERB will vigorously support the modernization of TCM and guide the rational discovery of modern medicines.

The research pattern of "why/how one TCM prescription treats one disease" can only allow us to study short-term and limited drug effects, such as anti-inflammatory effects or blood pressure reduction. It may also lead us to ignore many broader but profound effects of TCM prescriptions, such as heat clearing, detoxification, tranquilizing, anti-aging, and life-extending properties.

We have investigated TCM prescriptions that are proven to have remarkable curative effects, compared their components and genetic expressions with the Western medicine database CMap, and screened potential connections between gene targets and particular phenotypes [18]. To date, we have focused on Jian-yan-ling (JYL), a classic TCM prescription applied as a prognostic treatment after tumor radiotherapy and chemotherapy, effectively alleviating leukocytopenia. TCM prescriptions mainly consist of polygonum multiflorum (*Reynoutria multiflora* (Thunb.) Moldenke, root extraction), rhizoma polygonati (*Polygonatum kingianum* Collett & Hemsl., root extraction), astragalus membranaceus (*Astragalus mongholicu* Bunge, root extraction), radix asparagi (*Asparagus cochinchinensis* (Lour.) Merr., root extraction), dihuang (*Rehmannia glutinosa* (Gaertn.) DC., root extraction), chinese arborvitae (*Platycladus orientalis* (L.) Franco, twig extraction), amber, poria (*Wolfiporia cocos* (Schw.) Ryv. & Cilbn.), shanyao (*Dioscorea oppositifolia* L.), pearl, and sesame (*Sesamum indicum* L.).

The traditional use of JYL includes anti-aging, treatment of insomnia, and improving the quality of life of patients with tumors. The verifiable scientific references to the traditional use are as follows:

Drosophila melanogasters were cultured with 1% and 5% JYL drug dissolved in the medium (w/v), 10 h post-eclosion adults were collected. Adults were divided into groups by 100 and divided by sex, fed in an incubator at 28 °C. The survival number of *Drosophila* was counted every day, and the life span of the last dead adult in each group was the highest. The results showed that 1% JYL solution could prolong the half death day and average life expectancy of *Drosophila*. The average life span of male *Drosophila* was increased by 11.28% and that of female *Drosophila* was 11.63%, and the maximum life expectancy of male *Drosophila* was also prolonged. Similar

results were obtained with 5% JYL treatment. *Mus musculus* were orally fed JYL capsules at 250 mg/kg and 1500 mg/kg. After 97 days, blood was taken from abdominal aorta to determine SOD (Superoxide Dismutase) activity per gram of hemoglobin. The results showed that SOD activity in 250 mg/kg group was 30.98% higher than that in control group, and in 1500 mg/kg group that is 21.01% higher than in control group. The experiment shows that JYL does have the effect of prolonging life [14].

A clinical experiment on 82 cancer patients who are after radiotherapy or chemotherapy showed that the total effective rate of the treatment group (4 JYL capsules per time, 3 times a day) was 84.1%, which was significantly higher than that of the control group, 60.5% (chi-square test: $\chi^2 = 5.77$, $P < 0.025$). The results of the study showed that the ratio of CD4/CD8 of T-cell subsets of the patients after JYL treatment rebounded (0.98 ± 0.37 before treatment; 1.40 ± 9.0 after treatment), which was significantly higher than that of the control group (0.98 ± 0.37 before treatment; 92 ± 0.43, and 0.94 ± 0.33 after treatment). The results had a significant difference ($P < 0.01$), which means JYL could improve the cellular immune function of patients. JYL also can reduce the interleukin^2 receptor SIL-^{2}R in malignant tumor patients (668.6 ± 412.7 before treatment; 342.7 ± 101.3 after treatment), and the immune response returned to normal. Compared with the control group (701.5 ± 422.0 before treatment; 654.7 ± 325.8 after treatment), there is a significant difference ($P < 0.01$). The results of this study showed that JYL has a definite effect on leukopenia after radiotherapy and chemotherapy, and can enhance the immune function of patients [8].

The Pittsburgh Sleep Quality Index (PSQI) was used to evaluate the sleep quality of 360 patients with primary insomnia in a randomized, double-blind, double-simulated experiment. The results showed that treatment with JYL can reach 84.01% the total effective rate in primary insomnia [28].

The main purpose of this study was to explore the genetic mechanisms underlying the anti-aging and life-extending effects of JYL and its potential biological processes. *Drosophila melanogaster* was selected as the in vivo animal model because of its short lifespan. Flies also have three distinct life stages that allow us to examine the duration of the drug's effects and other information of interest. We selected Jurkat and HL-60 cell lines as candidates for in vitro experiments, as these humanized immune cell lines have both been widely used in various drug screening tests [1,6].

2. Material and methods

2.1. Reagents

JYL capsules (SFDA approval number: Z10950006; Batch number: TC17001; Quality control confirmed) were produced and provided by Suzhou Leiyunshang Medicine Pharmaceutical Co. Ltd. (Suzhou, China). The JYL drug powder was carefully triturated before use.

2.2. Animal treatment

Canton S *Drosophila* were raised at 25 °C and 60% relative humidity in a 14/10 h light/dark cycle on a standard *Drosophila* medium (water, cornmeal, agar, molasses, yeast, and nipagin). The JYL drug powder was dissolved in the medium to 4 mg/mL and 8 mg/mL for the low- (low-conc.) and high-concentration (high-conc.) groups, respectively with thorough stirring. The control group was treated with the standard *Drosophila* medium. We set up three vials, one each for the control group, the low-conc. Group (4 mg/mL JYL), and the high-conc. Group (8 mg/mL JYL). Thirty *Drosophila* eggs were placed in each vial, and the third instar larvae and adults 7 and 21 days post-eclosion were collected for RNA sequencing, irrespective of the gender. This sample number ensured sufficiency of samples, given the substantial mortality rate at all stages.

2.3. In vitro treatment

HL60 and Jurkat cell lines were seeded into 6-well-plates and allowed to adhere in DMEM culture media with 10% fetal bovine serum (Invitrogen, Carlsbad, CA, USA). Subsequently, the JYL drug powder mentioned above was thoroughly dissolved in cell culture media and filtered using 0.22 μm syringe filter (Millipore, USA). The final concentrations were 40 μg/mL and 80 μg/mL for the low and high concentration groups, respectively. The control group was cultured with the standard medium. Samples were incubated for 48 h before harvesting.

2.4. Total RNA extraction

Total RNA was extracted from the larvae, adult flies, and cells using TRIzol reagent (Invitrogen, Carlsbad, CA, USA) according to the manufacturer's instructions. For animals, approximately 60 mg of tissue was ground into powder using liquid nitrogen in a 2 mL tube, then homogenized for 2 min, and rested horizontally for 5 min. The mixture was centrifuged for 5 min at 12 000×*g* at 4 °C, and the supernatant was transferred into a new Eppendorf tube with 0.3 mL chloroform/isoamyl alcohol (24:1). The mixture was shaken vigorously for 15 s, and centrifuged at 12 000×*g* for 10 min at 4 °C. After centrifugation, the upper aqueous phase where RNA remained was transferred into a new tube with an equal volume of supernatant of isopropyl alcohol and then centrifuged at 12 000 *g* for 20 min at 4 °C. After removing the supernatant, the RNA pellet was washed twice with 1 mL 75% ethanol, and the mixture was centrifuged at 12 000 g for 3 min at 4 °C to collect the residual ethanol, then air dried for 5–10 min in a biosafety cabinet. Finally, 25–100 μL of DEPC-treated water was added to dissolve the RNA. Subsequently, the total RNA was quantified using a Nano Drop and Agilent 2100 bioanalyzer (Thermo Fisher Scientific, MA, USA).

For the mRNA library construction, oligo (dT)-attached magnetic beads were used to purify the mRNA. Purified mRNA was fragmented into small pieces using a fragment buffer at an appropriate temperature. First-strand cDNA was generated using random hexamer-primed reverse transcription followed by second-strand cDNA synthesis. Afterwards, A-Tailing Mix and RNA Index Adapters were added by incubating for end repair. The cDNA fragments obtained from the previous step were amplified by PCR, and products were purified using Ampure XP Beads and then dissolved in EB solution. The product was validated using an Agilent Technologies 2100 Bioanalyzer for quality control. The double-stranded PCR products from the previous step were denatured and circularized using splint oligo sequences to obtain the final library. Single-stranded circular DNA (ssCir DNA) was used as the final library. The final library was amplified with phi 29 to form a DNA nanoball (DNB), which had more than 300 copies of one molecule. DNBs were loaded into the patterned nanoarray and single end 50 base reads were generated on the BGIseq500 platform (BGI-Shenzhen, China).

2.5. Statistical analyses

Two-tailed Student's t-test was used to compare the differences between the groups. One-way analysis of variance (ANOVA) and factorial analysis were used to evaluate differences between more than two groups. SPSS 24.0, and GraphPad software packages (version 7.0) were used for image processing. In all cases, $P < 0.05$ was considered indicative of statistically significant differences.

3. Results

3.1. Drosophila

Differentially expressed genes (DEGs) in the *Drosophila* treatments were identified (Table 1) using sequencing and comparison analysis. The distribution of the DEGs between the treatments (Figs. 1 and 2) showed that for the *Drosophila* larvae and the d21 adults, the low-concentration (low-conc.) treatment had the most significant results, whereas for the d7 adult group the high concentrations (high conc.) had the most significant results. The low-conc. Group not only had a larger number of DEGs, but also more obvious effects, which predominantly consisted of the significant downregulation of genes. The high-conc. Group of the larvae showed no significant difference when compared with the control group.

Owing to significant differences in the low conc. Larvae group, KEGG pathway enrichment analysis was conducted and showed that various metabolic pathways were downregulated (Figs. 2 and 3). By comparing the DEGs from the different groups, a common

Table 1
Differentiated genes when compared with the control.

Group	Down	Up	Total
Low conc. Larvae	2315	74	2389
High conc. Larvae	5	3	8
Low conc. D7 adult	26	51	77
High conc. D7 adult	108	109	217
Low conc. D21 adult	4	115	119
High conc. D21 adult	3	12	15

Low conc.: 4 mg/mL JYL; High conc.: 8 mg/mL JYL; D7 adult: adult *Drosophila* 7 days post-eclosion; D21 adult: adult *Drosophila* 21 days post-eclosion.

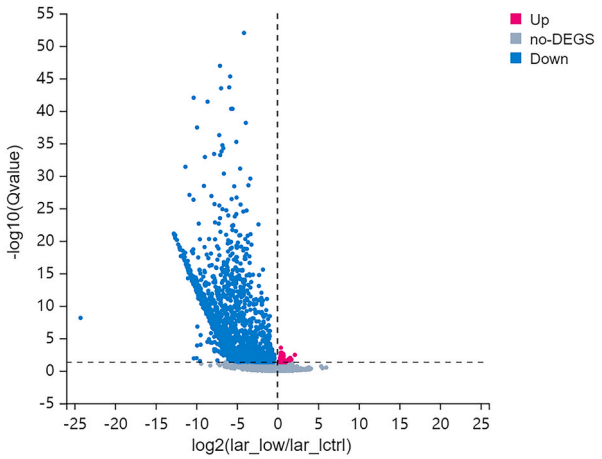

Fig. 1. Differentially expressed gene (DEG) distribution from the low conc. Larvae group.

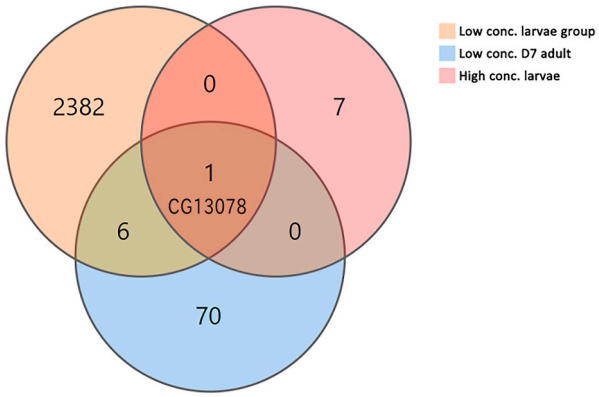

Fig. 2. VENN diagram showing the differentially expressed genes from the different treatment groups when compared with the control. Larvae group: third instar *Drosophila* larvae.

downregulated differential gene, CG13078 (NCBI gene ID: 35 251), was annotated. CG13078 is involved in the redox pathway and the synthesis of iron ascorbate reductase, a membrane protein that can achieve heme-binding activity and transmembrane ascorbate iron reductase activity. It is an ortholog of human CYB561D1 (cytochrome *b*561 family member D1) and CYB561D2 (cytochrome *b*561 family member D2). The cytochrome *b*561 family act as monodehydroascorbate reductases and $Fe^{[3+]}$ reductase, with ascorbic regeneration and transmembrane reduced iron transportation functions [2].

Further analysis of the co-expression map (Fig. 4) identified the top 10 key genes, as follows: regulatory particle non-ATPase (RPN), regulatory particle triple-A ATPase (RPT), and tripeptidyl-peptidase II (TPP II) (Fig. 5). The RPN gene family comprises a non-ATPase proteasome regulatory complex that encodes a component of the 26 S proteasome and degrades polyubiquitinated proteins in the cytoplasm and nucleus [3]. Previous studies have shown that this RPN family regulates cell apoptosis, autophagy, and the lifespan of adult *Drosophila* [10,12]. Upregulation of the RPN family may prolong the lifespan of adult *Drosophila* and alleviate obesity [17,21,22]. The RPT gene family is an ATP-dependent part of the 26 S proteasome [11], which acts as a proteolytic cascade downstream component of the 26 S proteasome in the ubiquitin-proteasome pathway [20]. By using MCODE, the subnetworks of the expression network were clustered to determine the possible upstream and downstream pathway relationships of key genes (Table 2). The results showed that all the key genes were in the first largest subnetwork. In summary, the JYL drug treatment may greatly increase the expression of 26 S proteasome components and their downstream genes (see Fig. 6).

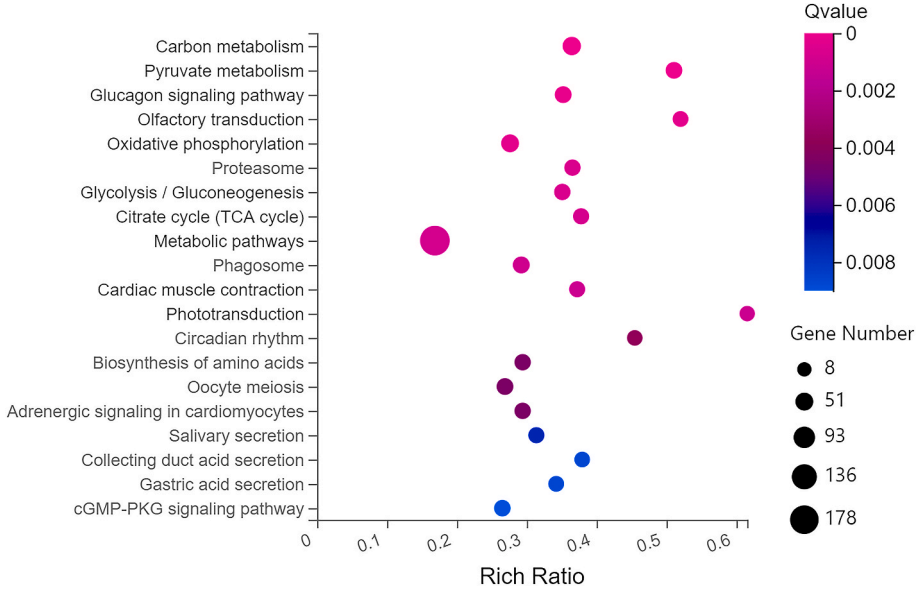

Fig. 3. KEGG pathway enrichment analysis of the low-conc. Larvae group. Top 20 pathways in KEGG enrichment by Q-Value. Rich factor is the ratio of the differentially expressed number of genes in the pathway and the total number of genes in the pathway. The higher the rich factor is, the higher the degree of enrichment. Q-Value is the *P*-value after the multiple hypothesis test correction, in the range of 0–1; the closer the Q-Value is to zero, the more significant the enrichment.

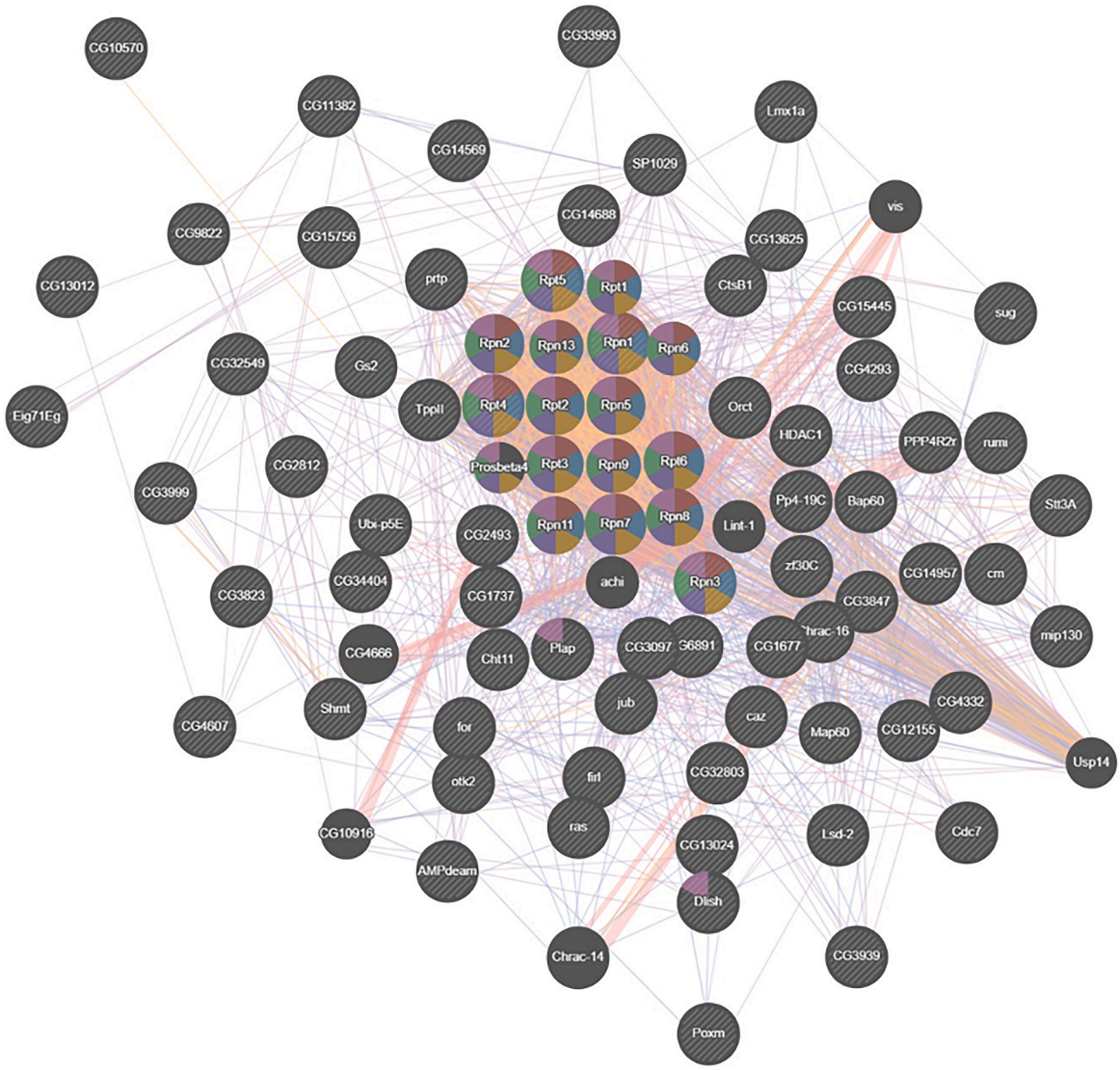

Networks

- Co-expression
- Physical Interactions
- Co-localization
- Predicted

Functions

- proteasome regulatory particle
- proteasome accessory complex
- proteasome complex
- endopeptidase complex
- peptidase complex
- proteasomal protein catabolic process

Fig. 4. Co-expression analysis and GO enrichment analysis for 74 genes that were up-regulated in the low-conc. Larvae group.

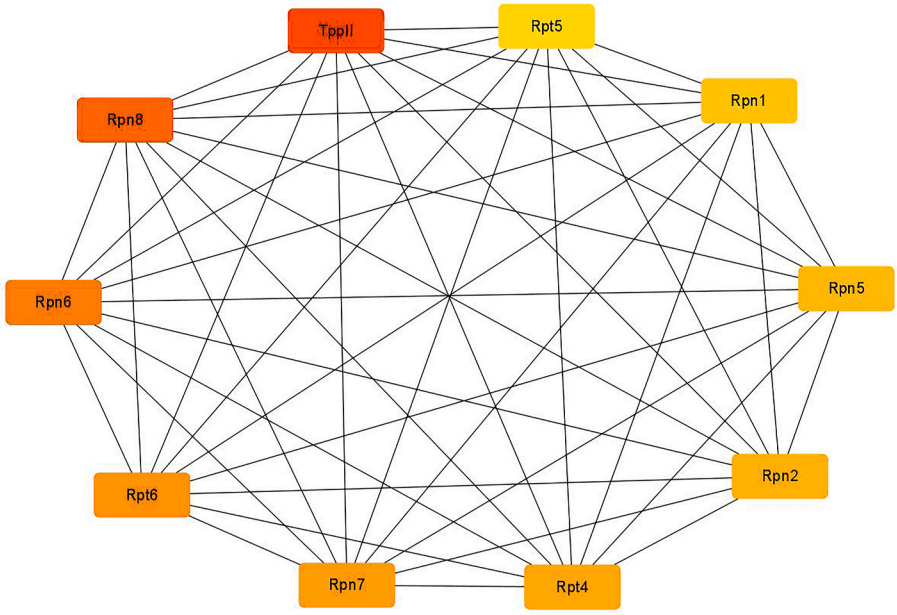

Fig. 5. Key upregulated genes in the low-conc. Larvae group. In anticlockwise direction, the boxes with colors ranging from red to yellow represent the genes in order from grade 1 to 10, and the edge represents the co-expression relationship. (For interpretation of the references to color in this figure legend, the reader is referred to the Web version of this article.)

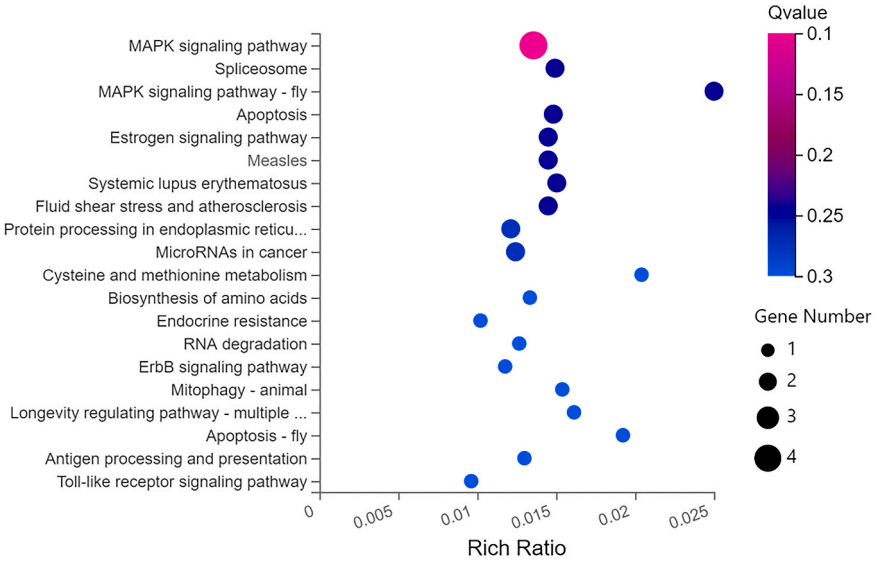

Fig. 6. KEGG pathway enrichment analysis of the HL60 cell line. Top 20 pathways in KEGG enrichment by Q-Value.

3.2. Human immune cell lines

The HL60 cell line showed the same characteristics as the JYL low conc. Larvae group (Table 3). Since the JYL drug was directly administered without undergoing drug metabolism, small drug molecules that can directly pass through the cell membrane should be the major factors responsible for gene expression changes.

For the cell line analysis, 19 co-differential genes were compared between different concentrations of the 60 cell line, of which three genes were upregulated: LOC107987457 (phostensin-like gene), HSPA1A (heat shock protein family A member 1 A), and H2AC19 (H2A clustered histone 19). Among these, there are currently no indications of the function of LOC107987457. However, HSPA1A is

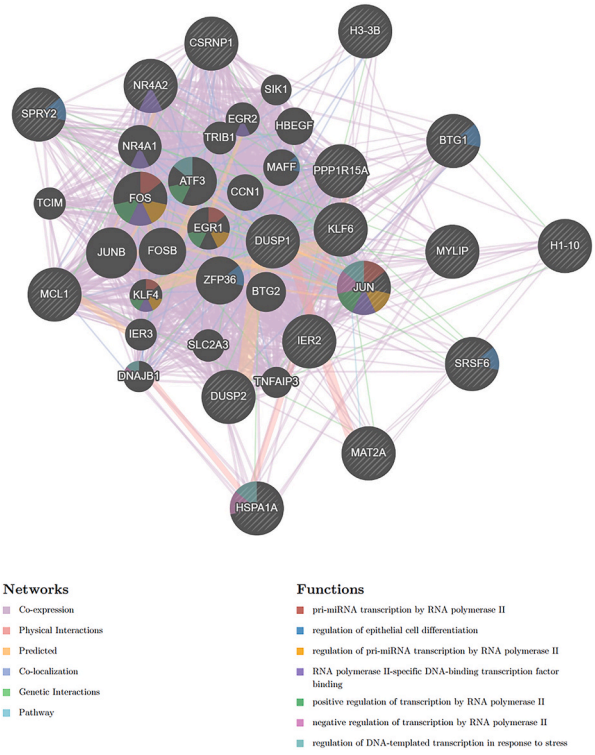

Fig. 7. Co-expression analysis and function enrichment of the HL60 cell line.

Table 2
Clustered sub-networks in the co-expression network.

Cluster	Nodes	Edges	Node IDs
1	24	2309	HDAC1, Rpn2, prtp, Rpn13, Rpt3, Rpt4, CG15445, Rpt6, Rpt5, Prosbeta4, TppII, Rpn8, Plap, Rpt1, Rpn1, Rpn6, Rpn11, Rpn7, Rpn3, Usp 14, Rpt2, Lint-1, Rpn5, Rpn9
2	13	55	SP1029, Lsd-2, Chrac-14, achi, CG32803, CG1677, for, Stt3A, PPP4R2r, mip130, zf30C, Shmt, CG3847
3	6	34	Map 60, CG1737, CG3097, Pp4-19C, Bap 60, CG12155
4	7	15	caz, CG3939, rumi, CG4293, jub, cm, Chrac-16

Table 3
Differentiated genes in the HL 60 cell line when compared with the control.

Group	Down	Up	Total
Low conc. HL60	162	263	425
High conc. HL60	18	4	22

known to encode a 70 kDa heat shock protein that stabilizes existing proteins to prevent aggregation and mediates the folding of newly translated proteins in the cytoplasm and organelles. It also participates in the ubiquitin-proteasome pathway by interacting with the AU-rich RNA binding proteins [16] Meanwhile the expression of HSPA1A helps specific immune system activation [5] and inhibits cancer cell metastasis [9]. H2AC19 is a member of the histone family and its expression has increased significantly (log2 (HL60_40/HL60_control) = 20.85; log2 (HL60_80/HL60_control) = 21.23). In the HL 60 cell line, JYL activated proteasome-related functions. In the Jurkat cell line, there were no common DEGs, despite the presence of a dosage-dependent trend.

We further investigated 19 genes in the HL 60 cell line using KEGG pathway and GO functional enrichment analyses. The main pathways included MAPK-related activation, proliferation, and apoptosis-related pathways. The representative upregulated gene was HSPA1A; the representative downregulated genes were SPRY2 (sprouty RTK signaling antagonist 2), DUSP1 (dual specificity phosphatase 1), JUN (Jun proto-oncogene, AP-1 transcription factor subunit), BTG1(B-cell translocation gene 1), and MCL1 (myeloid cell leukemia-1). SPRY2 is involved in the control of cell division [25], and its overexpression inhibits both cell growth and inflammation [27]. DUSP1 encodes a phosphatase with dual specificity for tyrosine and threonine residues. The DUSP1 encoded protein can dephosphorylate the MAP kinase MAPK1/ERK2, leading to its involvement in multiple cellular processes. This protein seems to play an

important role in the response of human cells to environmental stress and in the negative regulation of cell proliferation [19]. JUN is inhibited by the upregulation of the HSPA1A to prevent cell apoptosis and senescence [26]. The BTG1 (B-cell translocation gene 1) gene is a member of the anti-proliferative gene family that regulates cell growth and differentiation. The gene showed the highest expression during the G0/G1 phase, whereas it was downregulated after the G1 phase [15]. MCL1 encodes an anti-apoptotic protein that belongs to the Bcl-2 family. The longest gene product (isoform 1) enhances cell survival by inhibiting apoptosis, whereas shorter gene products (isoforms 2 and 3) may promote apoptosis and cell death [13]. From the KEGG pathway clustering, we found that the downregulation of these genes promoted cell proliferation and prevented cell apoptosis, predominantly through the MAPK pathway. From functional clustering, we have concluded that these genes predominately regulate the functions of RNA polymerase.

4. Discussion

According to the data derived from the *Drosophila* treated with JYL, iron ascorbate reductase expression was inhibited in all treatment groups in this study. Vitamin C is known to enter the mitochondria, where a large quantity of free radicals are produced via glucose transporter 1 (GLUT1), in the form of DHA [2]. In *Drosophila*, the biological processes associated with this gene (CG13078) are currently unclear and there is no available phenotypic data. However, the oxidation process associated with this gene is closely related to iron reduction, cellular anti-oxidation, and ferroptosis, but the specific effects of gene downregulation need to be investigated further. Through the analysis of upregulated genes, we found that JYL mainly acts on the protein ubiquitination decomposition pathway, promotes the production of protein enzyme bodies, and inhibits the effects of energy metabolism. Genes affected by JYL drugs have been shown to prolong the lifespan of adults is previous studies [14]. The JYL drug combination product, the 26s proteasome, has various proteolytic enzyme activities and is ubiquitin-dependent. It can directly affect the renewal of proteins, including those that play an important role in life activities. These functions are mainly involved in cell cycle control and apoptosis. The human immune cell lines in this investigation showed that the drug could also increase the production of protein enzymes, which may directly promote cell proliferation and inhibit cell apoptosis. From the above data, it can be inferred that the traditional Chinese medicine JYL may help to achieve a certain longevity and anti-aging effect by promoting the production of protein enzyme bodies, inhibiting energy metabolism, preventing cell apoptosis, and promoting cell proliferation. In addition, JYL may affect the intestinal microbial population of fruit flies, enabling the expansion of probiotics in female fruit flies.

To further explore the possible effective ingredients of the JYL drug, we conducted a CMap analysis and compared the expression profile data of this traditional Chinese medicine with the L1000 drug molecular expression profile database. The closest data to *Drosophila* larvae was for the drug cuneatin. This drug is currently used as a molecular activator of the Wnt/β-catenin pathway to reduce skin damage and treat metabolic disorders using disordered drugs and cytoskeleton modulators. The closest thing to the data from the HL cell line was the protein product processing of the UFD1L gene. The protein encoded by the UFD1L gene is necessary for the degradation of ubiquitinated proteins. The effects of the JYL Chinese medicine on human cells are predominately related to the degradation of ubiquitinated proteins. These results provide enlightenment to further improve our understanding of the specific active ingredients in traditional Chinese medicines.

The above-mentioned experiments and data show that the traditional Chinese medicine JYL has longevity and anti-aging effects, indicating that it is a traditional Chinese medicine which should be investigated further. Due to limitations in experimental conditions, the experimental scale used in the present study was insufficient. Expanding the scale of the experiment could reveal the detailed mechanisms underlying JYL's anti-aging effects.

Author contributions

Xiaobo Zhang: Conceptualization, Methodology, Formal analysis, Investigation, Writing - Original Draft.
Yunliang Zhai: Conceptualization, Methodology, Resources, Supervision.
Dandan Zhang: Software, Data Curation.
Chang Che: Validation, Visualization.
Yayun Zhang: Project administration.
Quan Li: Software, Formal analysis.
Xue Zhang: Writing - Review & Editing.
Lingrui Zhao: Validation, Resources, Writing - Review & Editing, Project administration.

Data availability statement

Data will be made available on request.

Additional information

Supplementary content related to this article has been published online at [URL].

Funding

This work was supported by the Key Laboratory of Growth Regulation and Translational Research of Zhejiang Province [grant number 2020E10027].

Declaration of competing interest

The authors declare that they have no known competing financial interests or personal relationships that could have appeared to influence the work reported in this paper

Acknowledgements

We sincerely thank our colleagues in the Key Laboratory of Growth Regulation and Translational Research of Zhejiang Province, School of Life Sciences, Westlake University for the assistance during the experiments. We also thank Lei Yun Shang Pharmaceutical Group Co., Ltd. Suzhou, China, who provided JYL capsules and quality control data for the experiments. Furthermore, we thank the BGI Group for their sequencing services. We also thank Editage (www.editage.cn) for English language editing.

Glossary

JYL	Jian-yan-ling, a drug used in traditional Chinese medicine (TCM)
TCM	traditional Chinese medicine
TCMID	Integrated Database of Traditional Chinese Medicine
HERB	Chinese medicine database for high-throughput experimental references
Control in vivo treatments	0 mg/mL JYL
Low conc. In vivo treatments	4 mg/mL JYL
High conc. In vivo treatments	8 mg/mL JYL
Larvae group	third instar larvae *Drosophila*
D7 adult	adult *Drosophila* 7 days post-eclosion
D21 adult	adult *Drosophila* 21 days post-eclosion
Control in vitro treatments	0 μg/mL JYL
Low conc. In vitro treatments	40 μg/mL JYL
High conc. In vitro treatments	80 μg/mL JYL
HL60	HL 60 cell line
DEG	differentially expressed gene
KEGG	Kyoto Encyclopedia of Genes and Genomes

References

[1] R.T. Abraham, A. Weiss, Jurkat T cells and development of the T-cell receptor signaling paradigm, Nat. Rev. 4 (2004) 301–307.
[2] H. Asard, R. Barbaro, P. Trost, A. Bérczi, Cytochromes b561: ascorbate-mediated trans-membrane electron transport, Antioxidants Redox Signal. 19 (2013) 1026–1035, https://doi.org/10.1089/ars.2012.5065.
[3] L. Budenholzer, C.L. Cheng, Y. Li, M. Hochstrasser, Proteasome structure and assembly, J. Mol. Biol. 429 (2017) 3500–3524, https://doi.org/10.1016/j.jmb.2017.05.027.
[4] S.S. Fang, L. Dong, L. Liu, et al., HERB: a high-throughput experiment and reference-guided data base of traditional Chinese medicine, Nucleic Acids Res. 49 (2020) D1197–D1206, https://doi.org/10.1093/nar/gkaa1063.
[5] C. Figueiredo, M. Wittmann, D. Wang, R. Dressel, A. Seltsam, R. Blasczyk, B. Eiz-Vesper, Heat shock protein 70 (HSP70) induces cytotoxicity of T-helper cells, Blood 113 (2009) 3008–3016, https://doi.org/10.1182/blood-2008-06-162727.
[6] R.A. Fleck, S. Romero-Steiner, M.H. Nahm, The HL-60 cell line was used to measure the opsonic capacity of the pneumococcal antibodies, Clin. Diagn. Lab. Immunol. 12 (2005) 19–27.
[8] Q. Jin, Li, Hanchong, Immune and anti-leukocytopenia effects of Jian-yan-ling treatment in post-radiotherapy and chemotherapy patients, J. Nanjing Med. University (natural sciences) 20 (2000) 155–156. https://kns.cnki.net/kcms/detail/detail.aspx?dbcode=CJFD&dbname=CJFD2000&filename=NJYK200002042&uniplatform=NZKPT&v=IPofU2JaztPfT75GkCBto-LXvafwHOwg5EY-tfphTU_aCDo0b98k_tCszF4CoF_L.
[9] P. Kasioumi, P. Vrazeli, P. Vezyraki, S. Zerikiotis, C. Katsouras, A. Damalas, C. Angelidis, Hsp70 (HSP70A1A) downregulation enhances the metastatic ability of cancer cells, Int. J. Oncol. 54 (2019) 821–832, https://doi.org/10.3892/ijo.2018.4666.
[10] L. Kovács, O. Nagy, M. Pál, A. Udvardy, O. Popescu, P. Deák, Role of the deubiquitylating enzyme DmUsp5 in coupling ubiquitin equilibrium to development and apoptosis in Drosophila melanogaster, PLoS One 10 (2015), e0120875, https://doi.org/10.1371/journal.pone.0120875.
[11] E. Kurucz, I. Andó, M. Sümegi, H. Hölzl, B. Kapelari, W. Baumeister, A. Udvardy, Assembly of the Drosophila 26 S proteasome is accompanied by extensive subunit rearrangement, Biochem. J. 365 (2002) 527–536, https://doi.org/10.1042/BJ20011520.
[12] S. Langerak, M.J. Kim, H. Lamberg, M. Godinez, M. Main, L. Winslow, M.B. O'Connor, C.C. Zhu, The Drosophila TGF-beta/activin-like ligands Dawdle and myoglianin appear to modulate adult lifespan through the regulation of 26S proteasome function in adult muscle, Biol. Open. 7 (2018), bio029454, https://doi.org/10.1242/bio.029454.
[13] U. Maurer, C. Charvet, A.S. Wagman, E. Dejardin, D.R. Green, Glycogen synthase kinase-3 regulates mitochondrial outer membrane permeabilization and apoptosis by destabilizing MCL-1, Mol. Cell. 21 (2006) 749–760, https://doi.org/10.1016/j.molcel.2006.02.009.

[14] Zengnian Qian, Z. Gu, E. Wang, et al., Pharmacologicalpharmacological study of the anti-aging effects of Jian-yan-ling capsules, Chin. Tradit. Herb. Drugs 19 (1988) 19–24. https://kns.cnki.net/kcms/detail/detail.aspx?dbcode=CJFD&dbname=CJFDLAST2018&filename=ZCYO198807011&uniplatform=NZKPT&v=sypRxsVcwAxVRQ69PYoW3xs9Bibe2zKY4RSCDuy_jPeg_f9yxqpQ86188K5wlUJW.
[15] J.P. Rouault, R. Rimokh, C. Tessa, G. Paranhos, M. ffrench, L. Duret, M. Garoccio, D. Germain, J. Samarut, J.P. Magaud, BTG1 is a member of a new family of anti-proliferative genes, EMBO J. 11 (1992) 1663–1670.
[16] J.H. Seo, J.H. Park, E.J. Lee, T.T. Vo, H. Choi, J.Y. Kim, J.K. Jang, H.J. Wee, H.S. Lee, S.H. Jang, Z.Y. Park, J. Jeong, K.J. Lee, S.H. Seok, J.Y. Park, B.J. Lee, M. N. Lee, G.T. Oh, K.W. Kim, ARD1-mediated Hsp70 acetylation balances stress-induced protein refolding and degradation, Nat. Commun. 7 (2016), 12882, https://doi.org/10.1038/ncomms12882.
[17] A. Simonsen, R.C. Cumming, A. Brech, P. Isakson, D.R. Schubert, K.D. Finley, Promoting basal levels of autophagy in the nervous system enhances longevity and oxidative resistance in adult Drosophila, Autophagy 4 (2008) 176–184, https://doi.org/10.4161/auto.5269.
[18] A. Subramanian, R. Narayan, S.M. Corsello, et al., A next generation connectivity map: L1000 platform and the first 1,000,000 profiles, Cell 171 (2017) 1437–1452, e17.
[19] H. Sun, C.H. Charles, L.F. Lau, N.K. Tonks, MKP-1 (3CH134), an immediate early gene product, is a dual-specificity phosphatase that dephosphorylates MAP kinases in vivo, Cell 75 (1993) 487–493, https://doi.org/10.1016/0092-8674(93)90383-2.
[20] B. Tomkinson, Tripeptidyl peptidase II: update on an old that still counts, Biochimie 166 (2019) 27–37, https://doi.org/10.1016/j.biochi.2019.05.012.
[21] A. Tonoki, E. Kuranaga, T. Tomioka, J. Hamazaki, S. Murata, K. Tanaka, M. Miura, Genetic evidence linking the age-dependent attenuation of the 26S proteasome with aging, Mol. Cell Biol. 29 (2009) 1095–1106, https://doi.org/10.1128/MCB.01227-08.
[22] E.N. Tsakiri, K.K. Iliaki, A. Höhn, S. Grimm, I.S. Papassideri, T. Grune, I.P. Trougakos, Diet-derived advanced glycation end products or lipofuscin disrupt proteostasis and reduce the lifespan of Drosophila melanogaster, Free Radic. Biol. Med. 65 (2013) 1155–1163, https://doi.org/10.1016/j.freeradbiomed.2013.08.186.
[23] Y. Tu, Artemisinin-A gift from traditional Chinese medicine to the world (nobel lecture), Angew Chem. Int. Ed. Engl. 55 (35) (2016) 10210–10226, https://doi.org/10.1002/anie.201601967.
[24] R. Xue, Z. Fang, M. Zhang, et al., TCMID: traditional Chinese medicine integrative database for herbal molecular mechanism analysis, Nucleic Acids Res. 41 (2013) D1089–D1095.
[25] Y. Yao, J. Luo, Y. Bian, Y. Sun, M. Shi, D. Xia, M. Niu, K. Zhao, L. Zeng, W. Chen, Z. Li, K. Xu, Sprouty2 regulates the proliferation and survival of multiple myeloma cells by inhibiting activation of the ERK1/2 pathway in vitro and in vivo, Exp. Hematol. 44 (2016) 474–482, https://doi.org/10.1016/j.exphem.2016.02.009, e2.
[26] S. Zhang, W. Liu, P. Wang, B. Hu, X. Lv, S. Chen, B. Wang, Z. Shao, HSP70 activation impedes tert-butyl hydroperoxide (t-BHP)-induced apoptosis and senescence of human nucleus pulposus stem cells by inhibiting the JNK/c-Jun pathway, Mol. Cell. Biochem. 476 (2021) 1979–1994, https://doi.org/10.1007/s11010-021-04052-1.
[27] W. Zhang, Z. Du, J. Zhu, J. Yu, Y. Xu, Sprouty2 suppresses inflammatory responses in rheumatoid arthritis fibroblast-like synoviocytes through regulating the Raf/ERK and PTEN/AKT signals, Mol. Immunol. 67 (2015) 532–539, https://doi.org/10.1016/j.molimm.2015.07.033.
[28] W. Zou, X.P. Yu, W. Teng, et al., Jian-yan-ling capsules for primary insomnia with kidney Yin deficiency: a multi-centered randomized double-blind and dummy controlled trial, Acta Chin. Med. Pharmacol. 43 (2015) 72–75, https://doi.org/10.19664/j.cnki.1002-2392.2015.02.022.